ACS APPLIED MATERIALS & INTERFACES

Research Article

www.acsami.org

Rational Design of Multiamphiphilic Polymer Compatibilizers: Versatile Solubility and Hybridization of Noncovalently Functionalized CNT Nanocomposites

Kie Yong Cho,[†,‡] Yong Sik Yeom,[†] Heun Young Seo,[†] Young Hun Park,[†] Ha Na Jang,[‡] Kyung-Youl Baek,[‡] and Ho Gyu Yoon*[,†]

[†]Department of Materials Science and Engineering, Korea University, Seoul 136-701, Korea

[‡]Materials Architecting Research Center, Korea Institute of Science Technology, 39-1 Hawolgok-dong, Seongbuk-gu, Seoul 136-791, Korea

Supporting Information

ABSTRACT: The design of amphiphilic polymer compatibilizers for solubility manipulation of CNT composites was systematically generalized in this study. Structurally tailored multiamphiphilic compatibilizer were designed and synthesized by applying simple, high-yield reactions. This multiamphiphilic compatibilizer was applied for noncovalent functionalization of CNTs as well as provided CNTs with outstanding dispersion stability, manipulation of solubility, and hybridization with Ag nanoparticles (NPs). With regard to the dispersion properties, superior records in maximum concentration (2.88−3.10 mg/mL in chloroform), and mass ratio of the compatibilizer for good CNT dispersion (36 wt %) were achieved by MWCNTs functionalized with a multiamphiphilic block copolymer compatibilizer. In particular, the solubility limitations of MWCNT dispersion in solvents ranging from toluene (nonpolar) to aqueous solution (polar) are surprisingly resolved by introducing this multiamphiphilic polymer compatibilizer. Furthermore, this polymer compatibilizer allowed the synthesis of the hybrid CNT nanocomposites with Ag nanoparticles by an in situ nucleation process. As such, the multiamphiphilic compatibilizer candidate as a new concept for the noncovalent functionalization of CNTs can extend their use for a wide range of applications.

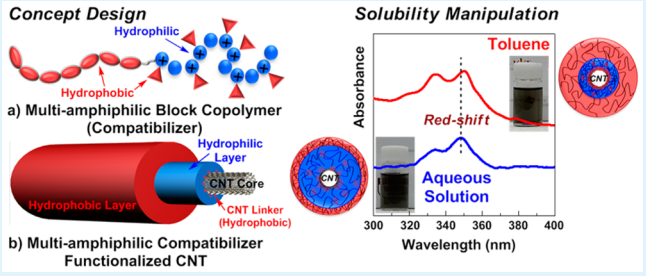

KEYWORDS: *amphiphilic block copolymer, carbon nanotube, noncovalent functionalization, solubility manipulation, nanocomposites, hybrid composites*

1. INTRODUCTION

The functionalization of carbon nanotubes (CNTs) has received substantial attention as a promising solution to overcome several limitations experienced by CNTs, related to the bundle state, solubility, processability, and compatibility.[1,2] Covalent functionalization is often considered as a simple but highly efficient method because the use of active species such as atoms, radicals, carbenes, nitrenes, or nitric/sulfuric acid could easily lead to favorable addition or oxidation reactions on the Stone−Wales defects of the CNT chemical structure.[3,4] Although the resulting products may exhibit highly effective dispersion in both solvents and matrix along with the introduction of various functional groups on the surface of the CNTs for postmodification reactions and to provide appropriate functionalities, reduction of the π-bonds on CNTs has been considered inevitable because of the severe chemical reaction conditions, as well as the low degree of functionalization of around 10%.[5] Furthermore, the destruction of π-bonds in the CNT chemical structure often leads to decline of its advantages conferred by its outstanding structural, electrical, thermal, and mechanical properties.[6]

In the next generation for functionalization of CNTs, noncovalent functionalization with polymer-type compatibilizers has attracted considerable interest as a promising candidate because of retention of the nature of the CNTs, along with the simpler and milder conditions. Moreover, such methods have been investigated in several reports to allow effective enhancement of the long-term dispersion stability, high concentration loading into solvents and matrixes while exhibiting a good dispersion state, and introduction of high-density functional groups on the surface of the CNTs.[7,8] However, to date, such studies have also revealed several drawbacks, including the following: (1) relatively low solubility and limited number of solvents for good dispersion and further use; (2) complicated and difficult synthesis methods are often required for preparation of the precursors and polymer compatibilizers; (3) large quantities of compatibilizers are generally required (approximately CNT:compatibilizer = 1:2

Received: March 1, 2015
Accepted: April 15, 2015
Published: April 15, 2015

DOI: 10.1021/acsami.5b01849
ACS Appl. Mater. Interfaces 2015, 7, 9841−9850

weight ratio); (4) lack of compatibility with other materials.[9−11] To this end, although tremendous endeavors have been made to overcome these shortcomings, problems still remain. Therefore, development of a solution remains as the next challenge for effective synthesis.

The first of the aforementioned issues could be solubility problems. If CNTs are capable of being dissolved at high concentrations with manipulation of the solubility in solvents ranging from polar to nonpolar, the high solubility may function to induce highly effective functionality and versatile compatibilities because larger loading of the CNTs with good miscibility readily leads to great enhancement in the range of performance manipulation; materials dissolved in both polar (water, methanol, etc.) and nonpolar (benzene, toluene, etc.) solvents are applicable in a variety of potential fields such as biotechnology, medicine, electronics, environmental, sensors, energy harvesting, and storage devices.[12−15] Second, the preparation of compatibilizer often takes a lot of time, and is achieved at low yield through difficult synthesis methods that require multisteps of modification reactions. Representative examples include P3HT copolymers, pyrene-functionalized polymers, functional acetylenes, and other conjugated polymers.[16−19] To this end, the development of polymer compatibilizers can be said to be a tedious task. Thus, easier, feasible, controllable, and high-yield reactions for the synthesis of compatibilizers should be suggested, such as simple addition reactions including conventional radical polymerization.[20,21] Third, the compatibilizer should be a minor component in the CNT composites when considering the favorable characteristics of the CNTs. To accomplish this, the functionalization of CNTs with minimum amounts of compatibilizer should be carried out by applying strong interfacial interactions between the CNT and compatibilizer, along with repulsive groups for sustaining a nonbundled state. Moreover, it is necessary to design compatibilizers containing components with good solubility. Fourth, the most common aim for compatibilizers should be to function as dispersants in CNT composites. However, the purpose of compatibilizer design can also go beyond general function, in which promising CNT composites could be induced by a postmodification strategy with utilization of CNTs and tertiary materials (NPs, QDs, ceramic, etc.) for the construction of hybrid composites.[22,23]

To date, the optimization of the compatibilizer design to meet the versatile CNT solubility has only been attempted by a few researchers with general ideas encompassing different polymer types (linear, star, and hyper-branch), block fractions, and various molecular weights.[24−28] However, this issue is still suffered from a lack of solubility and remained as a challenge. As a new approach, we propose a rational design of multiamphiphilic compatibilizers imbuing various functions on the CNTs. To accomplish this, pyrene-functionalized poly(methyl methacrylate)-poly(dimethylaminoethyl methacrylate) (PMMA−PDMAEMA) block and random types of two different copolymers were synthesized by the combination of atom transfer radical polymerization (ATRP) and simple amine quaternization. In the PMMA−PDMAEMA copolymers, the PMMA component worked as good soluble groups in various organic solvents and the spacer between functionalized CNTs to achieve retention of the nonbundled state, and the PDMAEMA component was applied for the water-soluble function after facile quaternization with the pyrene moiety. The functionalization of CNTs with amphiphilic compatibilizers often results in the development of three-dimensional structures. A hydrophobic inner layer generally encloses the CNT core, followed by the hydrophilic outer layer.[29−33] Meanwhile, CNT functionalization with the multiamphiphilic compatibilizer exhibited reverse alignment by the candidates of hydrophobic pendants in the hydrophilic inner layer, as shown in Scheme 1b. This new approach allowed a new type of the

Scheme 1. Schematic Depiction of Amphiphilic Compatibilizers; (a, b) Concept Images of Non-covalently Functionalized CNTs by General Amphiphilic Compatibilizer and Multiamphiphilic Compatibilizer, Respectively

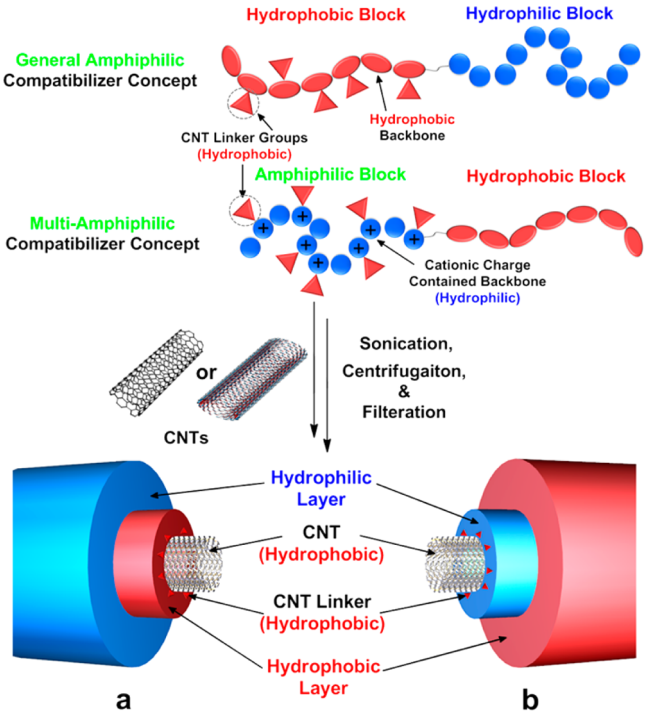

CNT interactive adhesion layer. This unique nanostructure formed by a new concept provided the versatile solubility covering solvent polarity indices ranging from 2.4 to 9 as well as superior dispersion properties involving high maximum concentration in chloroform (2.88−3.10 mg/mL) and long-term dispersion stability with the use of much reduced compatibilizer quantity (36 wt %). Furthermore, cationic charges on multiamphiphilic compatibilizers were utilized in fabrication of CNT-Ag NP hybrid composites by using electrostatic force. This function makes the multiamphiphilic compatibilizer more versatile than the general amphiphilic compatibilizer. To the best of our knowledge, this is the first report applying the multiamphiphilic compatibilizer concept for the noncovalent functionalization of CNTs, while achieving versatile solubility in solvents ranging from toluene to the aqueous solution, along with metal decoration enabling the expansion of potential applications.

2. EXPERIMENTAL SECTION

Materials. All reagents were purchased from Alfa Aesar and Sigma-Aldrich and applied as received, unless otherwise noted. Methyl methacrylate (MMA) and 2-(dimethylamino)ethyl methacrylate monomers were refined by distillation after removal of the moisture with calcium hydride.

DOI: 10.1021/acsami.5b01849
ACS Appl. Mater. Interfaces 2015, 7, 9841−9850

Scheme 2. Synthesis of Pyrene-Functionalized PMMA-*b*-PDMAEMA Block Copolymer

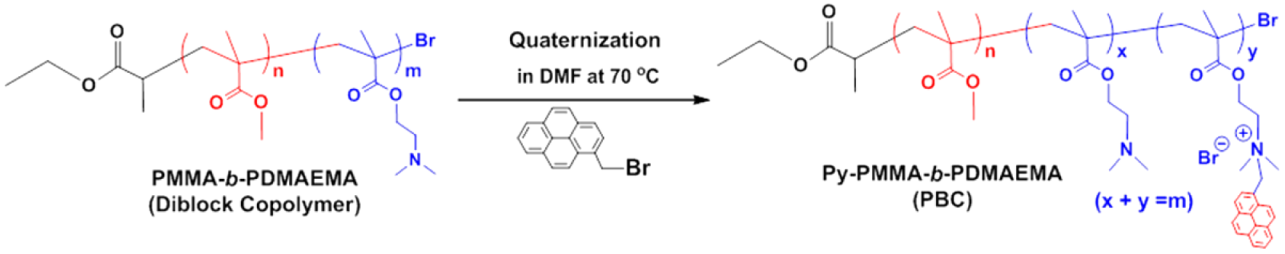

Characterization. The number-averaged molecular weight (M_n) and molecular weight distributions (M_w/M_n) of the samples were measured using a JASCO PU-2080 plus SEC system equipped with an RI-2031 and UV-2075 (254 nm detection wavelength) using THF as the eluent at 40 °C with a flow rate of 1 mL/min. The samples were separated through four columns: Shodex-GPC KF-802, KF-803, KF-804, and KF-805. ^{1}H NMR spectra were taken in $CDCl_3$ at 25 °C on a 300 MHz Varian Unity INOVA. UV−vis absorption spectra were measured in air with a JASCO V-670 spectrophotometer. Thermal gravimetric analysis (TGA) was performed with a TA Instruments (TGA 2950) under nitrogen using the heating rate of 10 °C min^{-1} from RT to 600 °C. The size distribution of Ag NPs was determined using dynamic light scattering (DLS) (Photal, ELSZ-1000) analysis after filtration through a 0.45 μm pore syringe filter. The PL experiments were carried out at room temperature in the range of 360−630 nm using a 350 nm excitation laser (Jasco, FP-6500). The X-ray diffraction patterns were acquired on a Rigaku diffractometer (Rigaku Smart Lab, Rigaku Co., Japan) operated at 45 kV and 40 mA with Cu$K\alpha$ radiation (λ = 1.5406 A°) and a diffracted beam monochromator. Data were collected between 2θ = 10° and 100° at 0.01° intervals. The phase was identified by matching each characteristic peak with the JCPDS files. Identification and characterization of functional groups were carried out using a Raman spectrometer (LabRam ARAMIS IR2, Horiba, Japan) with a laser at the excitation wavelengths of 532 nm (for MWCNT and its composites) and 785 nm (for SWCNT and its composites). The morphologies of pristine and functionalized CNTs were investigated by field-emission transmission electron microscopy (FE-TEM, Tecnai G2 F30 S-Twin, FEI Co., USA), carried out at an accelerating voltage of 300 kV.

Synthesis of Pyrene-Functionalized Block Copolymer Compatibilizer (PBC). The pyrene functionalization of PMMA-*b*-PDMAEMA block copolymer (PBC) was carried out by simple addition of 1-(bromomethyl)pyrene. PMMA-*b*-PDMAEMA copolymers (0.5 g) were added into a prebaked 100 mL RB flask and then 9.6 mL of DMF was sequentially injected. The solution was refluxed after connection of the condenser. Half an hour later, 1-(bromomethyl)-pyrene (0.16g, 0.056 mM) was added to the solution. The reaction was completed after 24 h. The conversion was measured by ^{1}H NMR analysis performed on samples directly taken from the reaction solution, which contained PBC and unreacted methyl pyrene (conversion: over 83.4%). The purification was performed simply by precipitation in 200 mL of hexane after removal of DMF, and then diluted with 10 mL of THF. The resultant was dried at RT for 48 h. ^{1}H NMR (300 MHz, $CDCl_3$, δ) (ppm): 7.9−8.4 (broad, pyrene), 5.2−5.7 (broad, 2H, NCH_2pyrene), 4.2−4.8 (broad, 2H, $OCH_2CH_2N(CH_3)_2(CH_2)_2$Pyrene), 4 (t, 2H, $OCH_2CH_2N(CH_3)_2$), 3.56 (s, 3H, OCH_3), 2.5 (t, 2H, $OCH_2CH_2N(CH_3)_2$), 2.3 (s, 6H, $OCH_2CH_2N(CH_3)_2$), 1.6−2.1 (broad, 2H, CH_2CCH_3 backbone), 0.7−1.3 (broad, 3H, CH_2CCH_3 backbone).

Synthesis of Multiamphiphilic Compatibilizer Functionalized CNTs. Ten milligrams of pristine CNTs was added to 90 mL of chloroform and then dispersed with the aid of mild sonication for 10 min. Upon completion of sonication, a prepared solution containing multiamphiphilic compatibilizer (30 mg) in chloroform (10 mL) was added to the CNTs dispersed in chloroform. The mixture was then sonicated for 30 min. The unreacted CNTs were removed by repeated centrifugation in chloroform, and the free multiamphiphilic compatibilizer was removed by several times of filtering with 0.2 μm pore filter paper after dilution with chloroform. The resultant was then redispersed in chloroform for further use.

Fabrication of Ag NP-Decorated PBCM Hybrid Composite. Ten milliliters of methanol solution containing 2 mg of PBCM was prepared with the aid of mild sonication for 2 min. A prepared 30 mL aqueous solution of sodium poly(acrylic acid) (SPAA) (0.33 mM) was then injected into the PBCM methanol solution, followed by vigorous agitation for 30 min. The $AgNO_3$ (0.2 mL, 0.05 mM) precursor aqueous solution was added to the solution containing SPAA-coated PBCM with vigorous stirring for 5 min. After completion of agitation, an aqueous solution of $NaBH_4$ (0.2 mL, 0.5 mM) reducing agent was slowly added to the above mixture under vigorous agitation for 30 min. Upon completion of the reaction, the crude solution was subjected to repeated centrifugations. The obtained Ag NPs decorated PBCM hybrid composite was eventually redispersed in 10 mL of water for the further use.

3. RESULTS AND DISCUSSION

3.1. Design and Synthesis of Multiamphiphilic Compatibilizer. Amphiphilic compatibilizers for the functionalization of CNTs have been introduced to manipulate the solubility of CNTs in various solvents to allow gratification of potential applications. To our knowledge, manipulation of the solubility to allow CNT composites to be dissolved in the range from toluene (polarity index: 2.4) to water (polarity index: 9) remains an unsolved task. Lei Zhai et al. tried to cope with this problem through the use of Poly(3-hexylthiophene)-*b*-poly(poly(ethylene glycol) acrylate) (P3HT-*b*-PPEGA) block copolymer.[30] Although water is a good solvent for PPEGA, the P3H-*b*-PPEGA functionalized CNT was not soluble in water. In addition, Gurkan Hizal et al. also joined the endeavor of solubility manipulation with examination of pyrene end functionalized polystyrene-*b*-poly(ethylene glycol)-*b*-poly(methyl methacrylate) miktoarm star polymer.[24] Although this material showed a wide solubility in toluene, chloroform, and DMF, it failed in the case of water. From these previous studies, we theorized two key points. First, the polarity of the hydrophilic groups was insufficient to allow dissolution of CNT in water. Second, the coordination of CNT and the hydrophobic anchor groups (P3HT and Pyrene/PS) in the interior CNT composite could generate extremely hydrophobic subdomains, resulting in a high surface tension with water. To that end, we modified and rearranged these concepts with the design of a multiamphiphilic compatibilizer. Following the assumptions above, the developed compatibilizer was supplemented by inclusion of highly polar cationic charges and hydrophobic pyrene groups in the PDMAEMA hydrophilic anchor block. Upon application of the multiamphiphilic compatibilizer, hydrophilic environments were formed around the CNTs with hydrophobic exterior layers, as shown in Scheme 1b. This minor tuning of the concept revealed release

DOI: 10.1021/acsami.5b01849
ACS Appl. Mater. Interfaces 2015, 7, 9841−9850

from the CNT solubility limitations. Furthermore, the cationic charges could be usefully applied for metal decoration on the surface of the CNTs through the electrostatic interaction, yielding CNT-NP hybrid composites.

To achieve this, we synthesized PMMA−PDMAEMA diblock copolymer and random copolymer using a conventional atom transfer radical polymerization (ATRP) reaction, as followed in Scheme S1 in the Supporting Information. The fraction of PDMAEMA in the block and random copolymer was 0.34 and 0.35, respectively, whereas the molecular weights measured by GPC were calculated to be 13k and 14k. The details of copolymer design parameters were optimized following the results of previous studies.[7,8,27] The simple quaternization reaction of amine groups in the PDMAEMA block was followed by the addition of 1-(bromomethyl)pyrene targeting 50% pyrene functionalization due to the solubility problems, as followed in Scheme 2. Figure 1 shows the ^{1}H

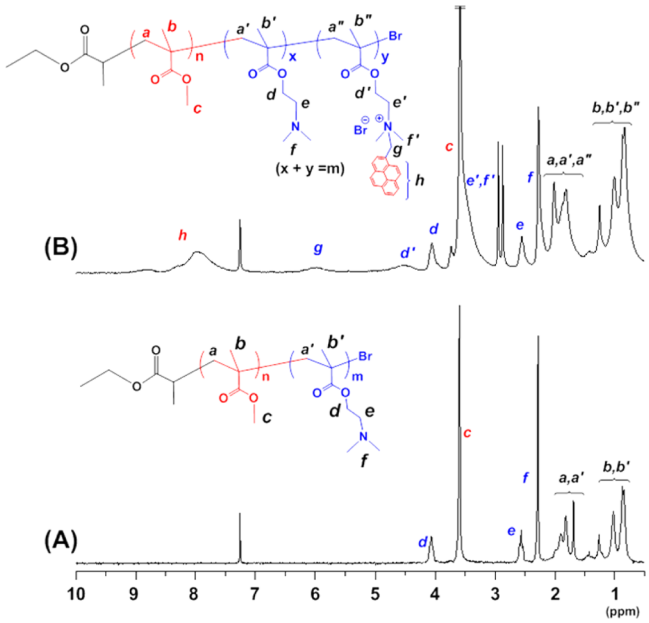

Figure 1. ^{1}H NMR spectra of (A) PMMA-*b*-PDMAEMA diblock copolymer and (B) pyrene-functionalized PMMA-*b*-PDMAEMA block copolymer compatibilizer in $CDCl_3$.

NMR spectra of PMMA-*b*-PDMAEMA and the pyrene-functionalized PMMA-*b*-PDMAEMA block copolymer compatibilizer (PBC). Dimethyl protons (*f*) and methylene protons (*d* and *e*) of the PDMAEMA absorption peaks were observed at 2.28, 4.06, and 2.56 ppm, respectively. After the addition of pyrene groups into the tertary amine, the peaks showed chemical shifts to 2.87 ppm (*f*′) and 2.94 ppm (*e*′) with a decrease of intensity, whereas the *d* of the methylene absorption peak was shifted in the broad range from 4.26 to 4.84 ppm (*d*′). The observed chemical shifts were applied to calculate the conversion of pyrene functionalization (41.7%). In Figure 1B, *g* and *h*, two broad peaks corresponding to methyl pyrene protons appeared in the range from 5.68 to 6.26 ppm and from 7.38 to 8.57 ppm, respectively. Pyrene-functionalized random copolymer (PRC) was synthesized and characterized for comparison (pryene functionalization: 48.6%, calculated from the ^{1}H NMR spectrum in Figure S3 in the Supporting Information). From these results, the chain length and number of pyrene groups were almost controlled, and comparison was made between the block and random copolymer compatibilizers (PBC and PRC, respectively).

3.2. Functionalized CNTs with Multiamphiphilic Compatibilizer. Multiamphiphilic compatibilizer functionalized MWCNTs were prepared while avoiding inclusion of unreacted reagents through multiple centrifugation and filtration steps, yielding PBC with MWCNT (PBCM) and PRC with MWCNT (PRCM). For the obtained composites, the formation of strong $\pi-\pi$ and cation$-\pi$ dual interactions was enabled by employment of pyrene moieties into the tertiary amine of PDMAEMA, functioning as interfacial linkers between the compatibilizer and MWCNT. Generally, $\pi-\pi$ stacking interactions are well-known strong interfacial noncovalent interactions formed between CNT and polymers. In particular, theoretical demonstration of these interactions indicated that conjugation groups located at the flexible position of the polymer resulted in higher adhesion characteristics in comparison to the stiff position.[34] As such, the anchor groups at the flexible side chain of PDMAEMA could be effectively approached along the CNT surface. Furthermore, the cationic charges on the quaternary ammonium groups enhanced the interfacial interaction to give stronger compatibilizer−CNT linkage.[35]

To confirm the strong and stable interfacial interactions between the compatibilizers and MWCNT, we performed transmission electron microscopy (TEM) and Raman spectroscopy analyses, as shown in Figure 2. In the TEM images of PBCM and PRCM composites, an increase of the diameter was observed in comparison to pristine MWCNT (7.7 nm) (Figure 2A). By comparison, PBCM exhibited a higher increase of the diameter, by about 10.83 nm than the 9.86 nm observed for PRCM. After introduction of the compatibilizers to MWCNTs, the resulting PBCM and PRCM composites showed good dispersion states, as shown in the right side of Figure 2A. In Figure S4 in the Supporting Information, the composites including PBC and PRC compatibilizers along with SWCNT (PBCS and PRCS) also exhibited change of diameter and good dispersion in an analogues manner as PBCM and PRCM. The typical Raman spectra were used to determine the interfacial interactions between the compatibilizers and CNTs. As shown in Figure 2B, the Raman spectrum of pristine MWCNT exhibited strong disorder-induced D and tangential G bands at 1344 and 1591 cm^{-1}, respectively. After being dispersed with the aid of the PBC or PRC, the both D and G bands of PBCM and PRCM shifted to lower wavenumbers of 1340 and 1586 cm^{-1}, respectively. As shown in Figure S5 in the Supporting Information, the tangential G band associated with the SWCNT metallic carbon showed a wavenumber shift from 1584 to 1589 cm^{-1} after functionalization with PBC and PRC compatibilizers. These Raman results of functionalized CNTs with compatibilizers exhibited the well-dispersed state of CNTs.[11,36]

The interfacial interactions between the pyrene moiety and CNT were examined to demonstrate the function of the pyrene groups. To accomplish this, UV−vis and PL emission analyses were carried out with the CNT-free compatibilizers and the functionalized CNTs. Figure 3A shows the typical UV−vis spectra of the PBC compatibilizer and the PBCM composite, prepared by dissolving in chloroform. In the spectrum of PBC, four strong absorption peaks were observed at 269.3, 279.9, 333.7, and 349.1 nm. After functionalization of the MWCNT with PBC, the UV−vis absorption peaks were red-shifted (approximately 2−3 nm), albeit the reduction of the peak

DOI: 10.1021/acsami.5b01849
ACS Appl. Mater. Interfaces 2015, 7, 9841−9850

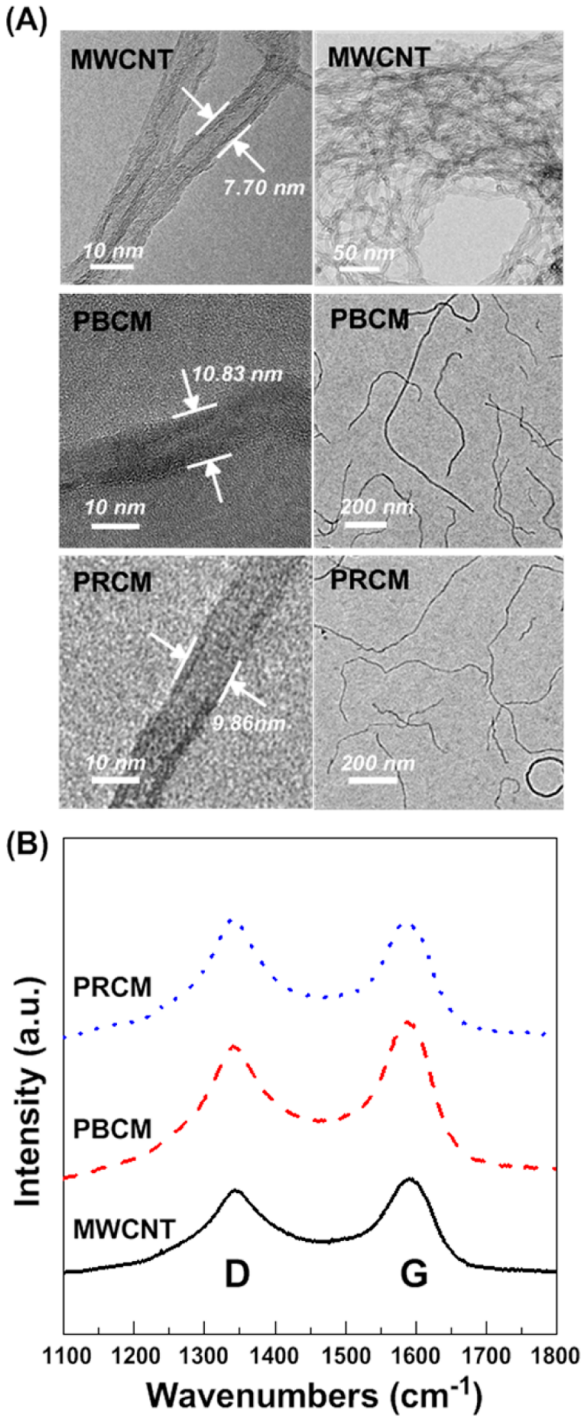

Figure 2. (A) TEM images and (B) Raman spectra of pristine MWCNT, PBCM, and PRCM.

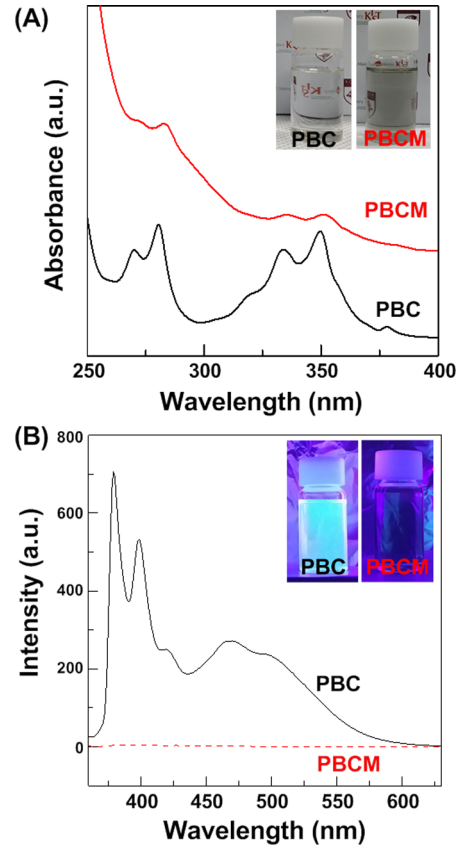

Figure 3. (A) UV−vis spectra of PBC and PBCM (inset: photographs of PBC and PBCM solutions in chloroform); (B) PL emission spectra of PBC and PBCM (inset: the photographs with irradiation with 350 nm light).

resolution. Moreover, this peak-shift behavior represented a stronger interfacial interaction between PBC and MWCNT than that in a previous report of a composite containing a pyrene group at the end of the polymer chain in which only reduced intensity without any peak shift was observed, corresponding to weak interfacial interaction between pyrene and MWCNT.[25] Figure 3B shows the typical PL emission spectra of PBC and PBCM. The excimer emission from the pyrene groups was significantly quenched after introduction of the MWCNT. This quenching effect could be understood as an energy transfer system from the pyrene donor to the MWCNT acceptor. The energy transfer behavior between conjugated polymers and CNTs has been observed in several reports.[29,32] In addition, the PL emission peak was shifted to lower wavelength about 1.4 nm, as shown in Figure S6C in the Supporting Information. This blue-shift could be attributed to the stable resonance of the ground state by $\pi-\pi$ interactions between PBC and MWCNT.[37] These results provided strong evidence for the interfacial interaction between the PBC and MWCNT. As shown in Figure S6A, B in the Supporting Information, the same photophysical behaviors were observed in the UV−vis and PL spectra of PRC and PRCM, clearly demonstrating that PRC formed an interfacial interaction with MWCNT.

3.3. Dispersion Properties. Obtaining noncovalently functionalized CNTs with a good dispersion state through minimum use of polymer compatibilizer has been demanded for effective reinforcement of the performances of CNTs as roles of electrical conductors, thermal conductors, chemical catalysts, sensors, capacitors, etc. This requirement could not be satisfied without optimized design of the polymer compatibilizer to involve strong interfacial interactions, proper repulsive moieties, and groups with good solubility. To that end, the newly developed multiamphiphilic compatibilizer was proposed as an appropriate material sufficiently meeting the functional requirements from the viewpoint of chemical structure.

Thermogravimetric analysis (TGA) curves were used to calculate the mass ratio between the compatibilizer and CNT in the functionalized CNTs, as well as to verify the functions of the multiamphiphilic compatibilizers. As can be seen in the

DOI: 10.1021/acsami.5b01849
ACS Appl. Mater. Interfaces 2015, 7, 9841−9850

TGA curves in Figure 4 and Figure S7 in the Supporting Information, abrupt large thermal degradation of MWCNT and

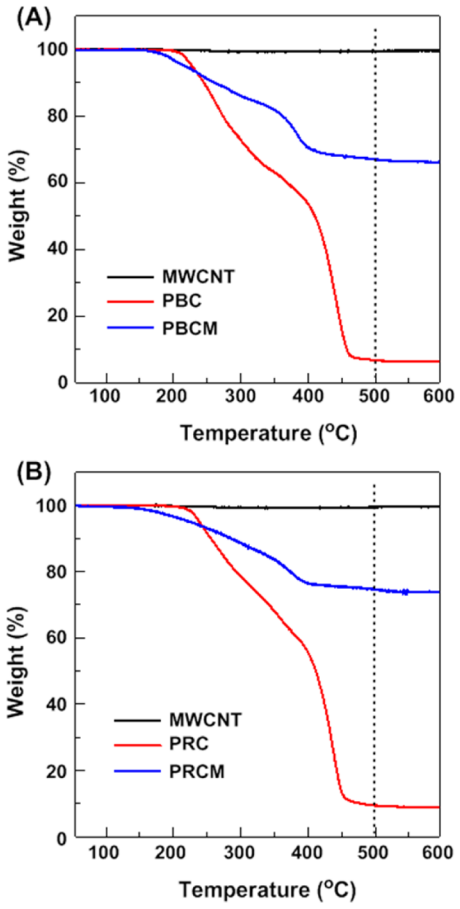

Figure 4. TGA weight loss curves of (A) pristine MWCNT, PBC, and PBCM; (B) pristine MWCNT, PRC, and PRCM.

SWCNT was not observed regardless of the temperature increase up to 600 °C, and both the compatibilizers (PBC and PRC) and functionalized CNTs (PBCM, PRCM, PBCS, and PRCS) showed equilibrium states at 500 °C. From these results, the mass ratio of the compatibilizer to CNTs could be deduced and defined from equation S1 in the Supporting Information. The calculated mass ratios are listed in Table 1. The samples listed in Table 1 can be compared according to the type of compatibilizers and CNTs. Block and random copolymer compatibilizers were applied for the functionalization of CNTs. Although they did not show large deviation, the block-type compatibilizer exhibited larger mass ratios of compatibilizer in comparison with the random type. This could be explained by examining the arrangement of pyrene moieties in the chemical structure of the compatibilizers, and was probably due to the broad distribution of pyrene moieties within the overall chain of the random copolymer, which could result in adhesion on the CNT surface with a lower number of compatibilizer chains compared to the block type. In comparison with SWCNT, the functionalization of MWCNT required a lower mass ratio of compatibilizer to allow good dispersion. It could be understood that the mass ratio of the compatibilizer is dependent on the dimensions and density of the CNTs, in which higher density and lower dimensions could lead to lower mass ratio of the compatibilizer. To examine this possibility, the diameters of the CNTs were determined from the TEM images, through which the MWCNT and SWCNT were measured to be about 7.7 and 11.4 nm, respectively. Furthermore, MWCNT generally showed a higher density than SWCNT. Consequently, MWCNT was well-dispersed with a lower mass ratio of compatibilizer compared to SWCNT. The results of the mass ratios were representative of the enhanced ability to disperse the CNTs with a lower mass ratio of polymer compatibilizers compared to some of the previous studies, in which the mass ratios of polymer compatibilizers to MWCNT were 50%.[8,24]

Table 1. Composite Mass Ratio and Maximum CNT Concentration in Chloroform

type	sample	mass ratio (CNT:compatibilizer)	maximum CNT concentration[a] (mg/mL)
multiamphiphilc	PBCM	64.0:36.0	2.88−3.10
	PRCM	71.7:28.3	0.11−0.15
	PBCS	49.8:50.2	1.15−1.28
	PRCS	56.2:43.8	0.08−0.1
amphiphilic	H-BCM	29.2:70.8	0.28−0.33

[a]The CNT composite solution in chloroform was concentrated until precipitates were observed.

One of the issues in CNT dispersion is obtaining the maximum concentration in the solvent while maintaining a good dispersion state. In the previous reports, the highest recorded value regarding of dispersing in organic solvents was around 3 mg/mL.[7,8] As shown in Table 1, the MWCNT functionalized with pyrene-functionalized block copolymer compatibilizer (PBCM) showed an almost identical maximum concentration (2.88−3.1 mg/mL) in chloroform. However, the MWCNT functionalized with pyrene-functionalized random copolymer compatibilizer (PRCM) showed a decrease by nearly 1 order of magnitude (0.11−0.15 mg/mL) in comparison to PBCM. In the case of the functionalized SWCNTs, the maximum CNT concentrations showed a similar trend to the MWCNTs. However, the observed maximum concentration of functionalized SWCNT was relatively lower because of the high dimensions of SWCNT. Comparison of the block- and random-type compatibilizers revealed that highly soluble groups of the CNTs functionalized with polymer compatibilizer should be extended from the surface of the CNT to allow dispersion of larger CNT concentrations in the solvent. The long-term dispersion stability in the solution state was examined at the dispersal concentrations of 0.2 mg/mL (for PBCS and PBCM) and 0.1 mg/mL (for PRCS and PRCM) in chloroform. As shown in Figure 5, the PBCS and PBCM continuously retained the typical dispersion state during a 7-month period, whereas the PRCS and PRCM exhibited precipitates at the bottom. Therefore, although the use of random-type compatibilizer demonstrated good dispersion of the CNTs with a lower mass ratio of the compatibilizer, the long-term dispersion stability in the solution-state indicated that the block-type compatibilizer was a better CNT dispersant because of the long extension of groups with good solubility, differing from the random-type compatibilizer (PRC).

Hydrogen-functionalized block copolymer compatibilizer (H-BC) was next prepared following Scheme S3A in the Supporting Information. The chemical structure of the H-BC obtained was characterized by ^{1}H NMR analysis, shown in Figure S8 in the Supporting Information, and it was used for

DOI: 10.1021/acsami.5b01849
ACS Appl. Mater. Interfaces 2015, 7, 9841−9850

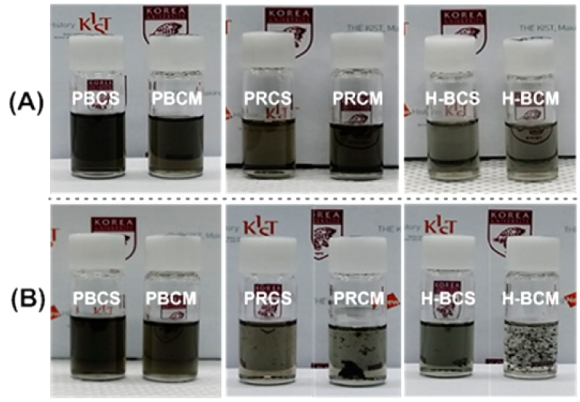

Figure 5. Typical photographs for the test of long-term dispersion stability in chloroform. (A) As-prepared solutions, (B) PBCS, PBCM, PRCS, and PRCM solutions after 7 months; H-BCS and H-BCM solutions after 1 week.

the functionalization of MWCNT following Scheme S3B in the Supporting Information. For comparison with the dispersion properties of PBCM and PRCM formed by dual interactions ($\pi-\pi$ and cation$-\pi$), examination was carried out of the composite mass ratio and maximum CNT concentration in chloroform for H-BCM, formed by only a single cation$-\pi$ interaction. The results were denoted in Table 1. The TGA analysis of H-BC in Figure S9 in the Supporting Information revealed that a much larger mass ratio of compatibilizer was required in comparison to PBCM. Moreover, the maximum CNT concentration of H-BCM in chloroform ranged from 0.28 to 0.33 mg/mL, demonstrating a decrease by almost one order of magnitude compared to PBCM. In Figure 5, the typical photographs showed affinity of the dispersion stability in chloroform. Although the H-BCM solution (0.1 mg/mL) showed a clear dispersion state in chloroform, precipitates were observed after 1 week. This was attributed to the aggregated or bundled state of MWCNT, originating from the weak interfacial interactions and difficulty of CNT adhesion because of the stiff position of the CNT interaction groups, which were observed and confirmed through TEM analysis in Figure S10 in the Supporting Information.

From the aforementioned dispersion properties, the following generalizations could be made about the optimization of compatibilizer design: (1) groups with good solubility in the polymer compatibilizer should be free to interact with other materials, such as solvents, polymer matrixes, and other third materials; (2) CNT surface adhesion or coverage are dependent on the number and location of CNT interaction groups; (3) long-term dispersion stability could be retained through having strong interfacial interactions with involvement of flexible groups with good solubility.

3.4. Solubility Manipulation. To demonstrate the solubility manipulation function, redispersion of the obtained composites was attempted in various solvents, including benzene, toluene, tetrahydrofuran, dichloromethane, chloroform, methanol, ethanol, dimethylformamide (DMF), and water. For the preparation of the PBCM solutions, the obtained PBCM solid was added to the each solvent and then followed mild sonication for 10 min. Most of the aforementioned solvents demonstrated appropriate dispersal of PBCM, as

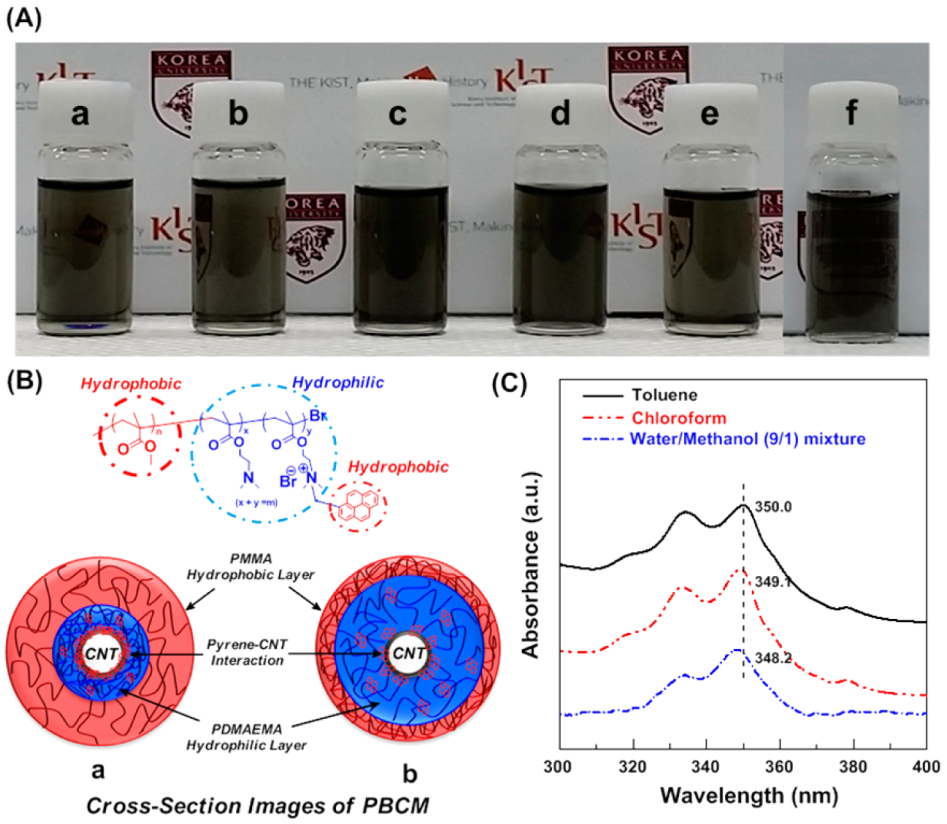

Figure 6. (A) Typical photographs of PBCM solutions in (a) toluene, (b) dichloromethane, (c) chloroform, (d) methanol, (e) DMF, and (f) water/methanol mixture (water/methanol = 9/1). (B) Schematic illustrations of PBCM cross-section in different solvents: (a) in toluene and (b) 9/1 water/methanol mixture. (C) UV–vis spectra of PBCM in different solvents (toluene, chloroform, and water/methanol (9/1) mixture).

DOI: 10.1021/acsami.5b01849
ACS Appl. Mater. Interfaces 2015, 7, 9841−9850

shown in Figure 6 A. However, although the PBC multiamphiphilic compatibilizer alone dissolved well in all of these solvents, PBCM was not easily soluble in water. It is worth mentioning that dispersal of 0.5 mg/mL PBCM in methanol was quick, observed after 5 min of mild sonication. A highly concentrated PBCM solution (1 mg/mL) in methanol was prepared, and then 9-fold vol % water was added. In the initial state, some precipitates were observed. However, after an hour of sonication, the precipitates disappeared and a stable dispersion state was formed, which was retained for at least several weeks. A photograph representing typical PBCM dispersion in the water/methanol (9/1) mixture is shown in Figure 6A,f.

This achievement regarding manipulation of the solubility in nonpolar to polar solvents could be explained from the viewpoint of composite structure, in that the multiamphiphilic compatibilizer functionalized MWCNT (PBCM) involved a hydrophilic PDMAEMA block with cationic charge in the interior and an hydrophobic PMMA block along with the pyrene hydrophobic anchor near the CNT surface. Cross-sectional images of the PBCM in different solvents (a. toluene and b. water/methanol mixture) were schematically illustrated in Figure 6B. In toluene, the interior hydrophilic layer was contracted near the surface of the CNT, while the exterior PMMA hydrophobic layer was fully spread out. Meanwhile, in the polar water/methanol (9/1) mixture, the interior cationic charge-containing hydrophilic layer underwent high amounts of swelling and expansion, resulting in the generation of hydrophilic circumstances around the CNT surface while the PMMA hydrophobic layer shrunk to form a very thin layer. This assumption, according to the description of the above illustration, was supported by analysis of the UV−vis spectra measured in different solvents, shown in Figure 6C. The main UV absorption peak in toluene (polarity index: 2.4) was observed at 350.0 nm, corresponding to the pyrene groups. As shown in Figure 6C, this peak underwent a blue-shift when solvents of higher polarity than chloroform (polarity index: 4.1, λ = 349.1 nm) were used, like the water/methanol (9/1) mixture (polarity index: 9/5.1, λ = 348.2 nm), indicating that the pyrene groups located at the side of the hydrophilic PDMAEMA appeared to drift apart. It is noteworthy that the above-mentioned blue-shift spanned a wide range of solvent polarities, with larger blue shifts observed for solvents with increasing polarity.[30] For comparison, solubility manipulation of the MWCNT functionalized with hydrogen-functionalized general amphiphilic compatibilizer (H-BCM) was also examined by dispersing in toluene, chloroform, methanol, and water. The H-BCM was readily dispersed in chloroform, methanol, and water, but not toluene, as shown in Figure S11 in the Supporting Information. We speculated that the influence of pyrene-functionalized multiamphiphilic compatibilizer (PBC) including both cationic charges and pyrene groups differed greatly from the H-BCM, containing only highly polar cationic charges, which inevitably limited the solubility in nonpolar solvents like toluene.

3.5. Ag NP−MWCNT Hybrid Nanocomposites. The cationic charges derived from the quaternized amines in the PDMAEMA block could provide a useful character for the postmodification strategy of the multiamphiphilic compatibilizer (PBC) because of the generation of noncovalent electrostatic interactions. In the previous works, metal nanoparticles generated by in situ nucleation process under electronegative environments were reported.[22,23,38] For example, polyether segments containing dendritic polymers or 2-(2ethoxyethoxy)ethoxy-modified polythiophene involving numerous electron-rich oxygen groups statically trapped the electropositive metal precursors. In that state, the metal precursors were nucleated and grown with the aid of the reducing agent $NaBH_4$. Those approaches motivated the decoration of PBC-functionalized MWCNT (PBCM) with Ag NPs herein.

Upon preparation of the PBCM water/methanol (9/1) solution, sodium poly(acrylic acid) (SPAA) solution in water was injected as a linker between the PBCM and Ag precursors. After agitating for half an hour, SPAA-coated PBCM was fabricated, as shown in Figure 7A,a. An $AgNO_3$ solution prepared in water was added to the SPAA-coated PBCM, after which the Ag precursors were trapped by electrostatic interaction. When $NaBH_4$ reducing agent was added, nucleation of the Ag precursors occurred. The Ag NP-decorated PBCM hybrid composite was finally obtained, as shown in Figure 7A,b. After purification through centrifugation with water several times, the obtained hybrid composites were redispersed in water. The solubility manipulation test was then performed by attempting to dissolve the products in chloro-

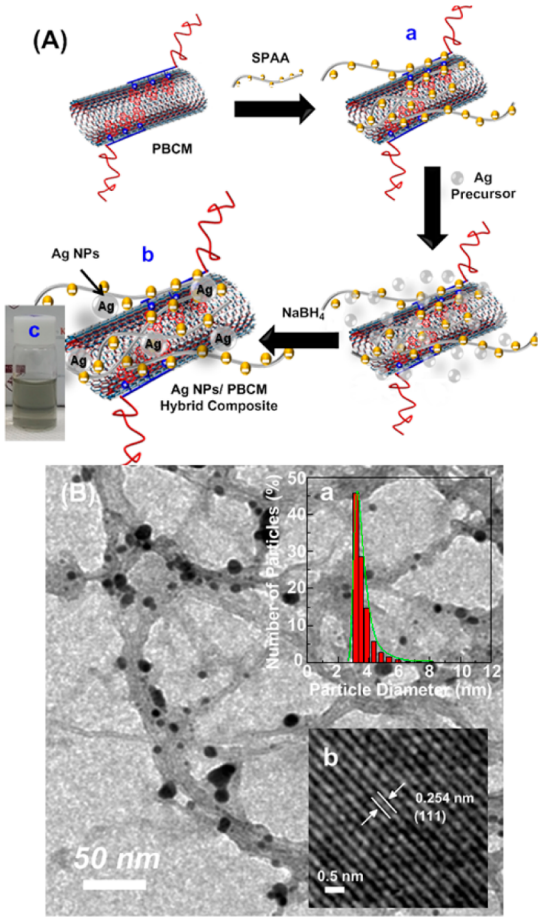

Figure 7. (A) Schematic illustration for a fabrication of Ag NP decoration on the surface of PBCM: (a) PBCM-coated by sodium poly(acrylic acid) (SPAA), (b) Ag NP decoration on the surface of PBCM by SPAA linker (Ag NPs/PBCM hybrid composite), and (c) typical photograph of redispersed Ag NPs/PBCM hybrid composite in water. (B) TEM image of Ag NPs/PBCM hybrid composite: (a) size distribution of Ag NPs in water and (b) crystal lattice with spacing of 0.254 nm and consistent with Ag crystal plane of (111).

DOI: 10.1021/acsami.5b01849
ACS Appl. Mater. Interfaces 2015, 7, 9841−9850

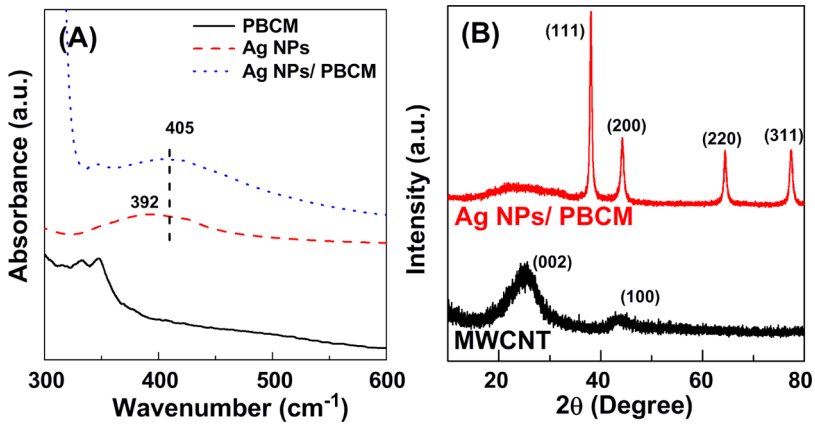

Figure 8. (A) UV−vis spectra of PBCM, Ag NPs, and Ag NP/PBCM hybrid composite dissolved in water/methanol (9:1) mixture; (B) XRD patterns of pristine MWCNT and Ag NP/PBCM hybrid composite.

form, THF, methanol, and water. The hybrid composites with Ag NPs demonstrated complete change of the solubility properties, and could be dissolved only in polar solvents such as methanol and water. It can be explained that SPAA was only soluble in water, and not in any organic solvents. Figure 7A,c shows a typical photograph of the Ag NPs/PBCM hybrid composite solution in water, indicating good solubilization in water.

The decoration of Ag NPs on the surface of the PBCM was confirmed by TEM. In Figure 7B, a few nanosized Ag NPs were ornamented along the SPAA-coated PBCM wall. As shown in Figure 7B,a, the sizes of the Ag NPs ranged from 3 to 8 nm, as determined by dynamic light-scattering (DLS) in water. However, some Ag NPs of larger size were observed in the TEM image of Figure 7. In fact, the conditions for the control of nanoparticle size distribution are still under investigation with the change of SPAA quantity, since that aggregation of Ag NPs can depend on the interaction between SPAA and the Ag precursors. Several TEM images of the Ag NPs/PBCM hybrid composite are shown in Figure S12 in the Supporting Information. The TEM images demonstrated that a number of Ag NPs were attached on the fairly dispersed PBCM, except for the image in Figure S12A in the Supporting Information. Aggregation of the PBCM may occur because of the role of SPAA, which is often noncovalently cross-linked between PBCMs. Furthermore, energy-dispersive X-ray spectroscopy (EDS) analysis was conducted to confirm the Ag NP component on the PBCM in Figure S13 in the Supporting Information. As shown in Figure S13B in the Supporting Information, the EDS analysis of the red points on the dark-field TEM image represented the silver component.

UV−vis and XRD analysis were also used for verification of the structure of the Ag NPs/PBCM hybrid composites in Figure 8. UV−vis analysis of the Ag NPs revealed a broad absorption peak for Ag NPs of less than 10 nm in size, observed in Figure 8A. After formation of the Ag NP/PBCM hybrid composite, the absorption peak showed a red shift from 392 to 405 cm^{-1}, indicating that the Ag NPs aggregated and interacted with MWCNT. The XRD spectra in Figure 8B showed the XRD pattern of Ag NPs corresponded to face-centered cubic (FCC) structure. Moreover, the d-spacing of the Ag nanoparticles in the (111) plane was determined with the d-spacing equation $(2\pi/q)$ by using the q value deduced from the equation $\sin\theta = q\lambda/4\pi$, where q is the scattering vector and λ is the wavelength. The d-spacing value was calculated to be 0.267 nm, which was almost consistent with that measured from the crystal lattice of the Ag NPs TEM image (0.254 nm) in Figure 8B,b. Therefore, the decoration of Ag NPs on PBCM was successful, and this hybrid composite could lead to the expansion of potential applications for CNTs.

4. CONCLUSIONS

Multiamphiphilic polymer compatibilizers were successfully designed and synthesized for the noncovalent functionalization of CNTs. The obtained functionalized CNTs showed great dispersion in chloroform despite containing relatively low mass ratios of the compatibilizers. The pyrene-functionalized block copolymer compatibilizer (PBC) functionalized MWCNT (PBCM) in particular achieved long-term dispersion stability in the solution state compared to PRCM and H-BCM, while showing high MWCNT concentration in chloroform (2.88−3.10 mg/mL) comparable to the highest value reported so far. Through rational design and tailoring of the dispersion properties of PBC, we were able to attain surprisingly versatile solubility ranging from toluene (nonpolar) to aqueous solution (polar), fully differed from general amphiphilic compatibilizers. In addition, the PBCM composites were well-decorated with Ag NPs through a facile in situ nucleation process with the aid of SPAA interfacial linker.

■ ASSOCIATED CONTENT

Supporting Information

Details of synthetic materials; Figures S1−S15 and equation S1 as mentioned in the main text. This material is available free of charge via the Internet at http://pubs.acs.org.

■ AUTHOR INFORMATION

Corresponding Author

*E-mail: hgyoon@korea.ac.kr. Tel: +82-2-3290-3277. Fax: +82-2-928-3584.

Notes

The authors declare no competing financial interest.

■ ACKNOWLEDGMENTS

This work was supported by the Industrial Strategic Technology Development Program, (Project 10041829, Development of Prototype 154 kV Compact Power Cables with Insulation Thickness Decreased by 15% or More Based on Ultrasupersmooth Semiconductive Materials) funded by the

DOI: 10.1021/acsami.5b01849
ACS Appl. Mater. Interfaces 2015, 7, 9841−9850

Ministry of Trade, Industry & Energy (MI, Korea) and partially supported by a grant from the Fundamental R&D Program for Core Technology of Materials funded by the Ministry of Knowledge Economy, Republic of Korea.

REFERENCES

(1) Hirsch, A. Functionalization of Single-Walled Carbon Nanotubes. *Angew. Chem., Int. Ed.* **2002**, *41*, 1853−1859.
(2) Bahr, J. L.; Tour, J. M. Covalent Chemistry of Single-Wall Carbon Nanotubes. *J. Mater. Chem.* **2002**, *12*, 1952−1958.
(3) Balasubramanian, K.; Burghard, M. Chemically Functionalized Carbon Nanotubes. *Small* **2005**, *1*, 180−192.
(4) Kim, Y. J.; Shin, T. S.; Choi, H. D.; Kwon, J. H.; Chung, Y.-C.; Yoon, H. G. Electrical Conductivity of Chemically Modified Multiwalled Carbon Nanotube/Epoxy Composites. *Carbon* **2005**, *41*, 23−30.
(5) Dyke, C. A.; Tour, J. M. Overcoming the Insolubility of Carbon Nanotubes through High Degrees of Sidewall Functionalization. *Chem.—Eur. J.* **2004**, *10*, 812−817.
(6) Liu, P. Modifications of Carbon Nanotubes with Polymers. *Eur. Polym. J.* **2005**, *41*, 2693−2703.
(7) Meuer, S.; Braun, L.; Schilling, T.; Zentel, R. α-Pyrene Polymer Functionalized Multiwalled Carbon Nanotubes: Solubility, Stability and Depletion Phenomena. *Polymer* **2009**, *50*, 154−160.
(8) Zou, J.; Liu, L.; Chen, H.; Khondaker, S. I.; McCullough, R. D.; Huo, Q.; Zhai, L. Dispersion of Pristine Carbon Nanotubes Using Conjugated Block Copolymers. *Adv. Mater.* **2008**, *20*, 2055−2060.
(9) Chen, J.; Liu, H.; Weimer, W. A.; Halls, M. D.; Waldeck, D. H.; Walker, G. C. Noncovalent Engineering of Carbon Nanotube Surfaces by Rigid, Functional Conjugated Polymers. *J. Am. Chem. Soc.* **2002**, *124*, 9034−9035.
(10) Cui, K. M.; Tria, M. C.; Pernites, R.; Binag, C. A.; Advincula, R. C. PVK/MWNT Electrodeposited Conjugated Polymer Network Nanocomposite Films. *ACS Appl. Mater. Interfaces* **2011**, *3*, 2300−2308.
(11) Tasis, D.; Mikroyannidis, J.; Karoutsos, V.; Galiotis, C.; Papagelis, K. Single-Walled Carbon Nanotubes Decorated with a Pyrene−Fluorenevinylene Conjugate. *Nanotechnology* **2009**, *20*, 135606.
(12) Katz, E.; Willner, I. Biomolecule-Functionalized Carbon Nanotubes: Applications in Nanobioelectronics. *ChemPhysChem* **2004**, *5*, 1084−1104.
(13) Baughman, R. H.; Zakhidov, A. A.; de Heer, W. A. Carbon Nanotubes—the Route Toward Applications. *Science* **2002**, *297*, 787−792.
(14) Fabbro, C.; Ali-Boucetta, H.; Ros, T. D.; Kostarelos, K.; Bianco, A.; Prato, M. Targeting Carbon Nanotubes Against Cancer. *Chem. Commun.* **2012**, *48*, 3911−3926.
(15) Dai, L.; Chang, D. W.; Baek, J.-B.; Lu, W. Carbon Nanomaterials for Advanced Energy Conversion and Storage. *Small* **2012**, *8*, 1130−1166.
(16) Park, H. S.; Choi, B. G.; Hong, W. H.; Jang, S. Y. Interfacial Interactions of Single-Walled Carbon Nanotube/ Conjugated Block Copolymer Hybrids for Flexible Transparent Conductive Films. *J. Phys. Chem. C* **2012**, *116*, 7962−7967.
(17) Sun, J. Z.; Qin, A. J.; Tang, B. Z. Functional Polyacetylenes: Hybrids with Carbon Nanotubes. *Polym. Chem.* **2013**, *4*, 211−223.
(18) Imin, P.; Cheng, F.; Adronov, A. Supramolecular Complexes of Single Walled Carbon Nanotubes with Conjugated Polymers. *Polym. Chem.* **2011**, *2*, 411−416.
(19) Tuncel, D. Non-Covalent Interactions between Carbon Nanotubes and Conjugated Polymers. *Nanoscale* **2011**, *3*, 3545−3554.
(20) Cho, K. Y.; Hwang, S. S.; Yoon, H. G.; Baek, K.-Y. Electroactive Methacrylate-Based Triblock Copolymer Elastomer for Actuator Application. *J. Polym. Sci., Part A: Polym. Chem.* **2013**, *51*, 1924−1932.
(21) Cho, K. Y.; Choi, J. W.; Lee, S. H.; Hwang, S. S.; Baek, K. Y. Thermoresponsive Amphiphilic Star Block Copolymer Photosensitizer: Smart BTEX Remover. *Polym. Chem.* **2013**, *4*, 2400−2405.
(22) Li, H.; Cooper-White, J. J. Hyperbranched Polymer Mediated Fabrication of Water Soluble Carbon Nanotube−Metal Nanoparticle Hybrids. *Nanoscale* **2013**, *5*, 2915−2920.
(23) Li, H.; Jo, J. K.; Zhang, L.; Ha, C.-S.; Suh, H.; Kim, I. A General and Efficient Route to Fabricate Carbon Nanotube-Metal Nanoparticles and Carbon Nanotube-Inorganic Oxides Hybrids. *Adv. Funct. Mater.* **2010**, *20*, 3864−3873.
(24) Durmaz, H.; Dag, A.; Tunca, U.; Hizal, G. Synthesis and Characterization of Pyrene Bearing Amphiphilic Miktoarm Star Polymer and Its Noncovalent Interactions with Multiwalled Carbon Nanotubes. *J. Polym. Sci., Part A: Polym. Chem.* **2012**, *50*, 2406−2414.
(25) Assali, M.; Leal, M. P.; Fernandez, I.; Romero-Gomez, P.; Baati, R.; Khiar, N. Improved Non-Covalent Biofunctionalization of Multi-Walled Carbon Nanotubes Using Carbohydrate Amphiphiles with a Butterfly-Like Polyaromatic Tail. *Nano Res.* **2010**, *3*, 764−778.
(26) Lou, X.; Daussin, R.; Cuenot, S.; Duwez, A.-S.; Pagnoulle, C.; Detrembleur, C.; Bailly, C.; Jerome, R. Synthesis of Pyrene-Containing Polymers and Noncovalent Sidewall Functionalization of Multiwalled Carbon Nanotubes. *Chem. Mater.* **2004**, *16*, 4005−4011.
(27) Meuer, S.; Braun, L.; Zentel, R. Pyrene Containing Polymers for the Non-Covalent Functionalization of Carbon Nanotubes. *Macromol. Chem. Phys.* **2009**, *210*, 1528−1535.
(28) Kim, B.-S.; Kim, D.; Kim, K.-W.; Lee, T.; Kim, S.; Shin, K.; Chun, S.; Han, J. H.; Lee, Y. S.; Paik, H.-J. Dispersion of Non-Covalently Functionalized Single-Walled Carbon Nanotubes with High Aspect Ratios using Poly(2-dimethylaminoethyl methacrylate-co-styrene). *Carbon* **2014**, *72*, 57−65.
(29) Kim, K. T.; Jo, W. H. Synthesis of Poly(3-hexylthiophene)-graft-poly(t-butyl acrylate-co-acrylic acid) and its Role of Compatibilizer for Enhancement of Mechanical and Electrical Properties of Nylon 66/ Multi-Walled Carbon Nanotube Composites. *Compos. Sci. Technol.* **2009**, *69*, 2205−2211.
(30) Zou, J.; Khondaker, S. I.; Huo, Q.; Zhai, L. A General Strategy to Disperse and Functionalize Carbon Nanotubes Using Conjugated Block Copolymers. *Adv. Funct. Mater.* **2009**, *19*, 479−483.
(31) Kim, K. T.; Jo, W. H. Non-Destructive Functionalization of Multi-Walled Carbon Nanotubes with Naphthalene-Containing Polymer for High Performance Nylon66/Multi-Walled Carbon Nanotube Composites. *Carbon* **2011**, *49*, 819−826.
(32) Mandal, A.; Nandi, A. K. Noncovalent Functionalization of Multiwalled Carbon Nanotube by a Polythiophene-Based Compatibilizer: Reinforcement and Conductivity Improvement in Poly(vinylidene fluoride) Films. *J. Phys. Chem. C* **2012**, *116*, 9360−9371.
(33) White, B.; Banerjee, S.; O'Brien, S.; Turro, N. J.; Herman, I. P. Zeta-Potential Measurements of Surfactant-Wrapped Individual Single-Walled Carbon Nanotubes. *J. Phys. Chem. C* **2007**, *111*, 13684−13690.
(34) Yang, M.; Koutsos, V.; Zaiser, M. Interactions between Polymers and Carbon Nanotubes: A Molecular Dynamics Study. *J. Phys. Chem. B* **2005**, *109*, 10009−10014.
(35) Wang, S.; Yu, D.; Dai, L. Polyelectrolyte Functionalized Carbon Nanotubes as Efficient Metal-free Electrocatalysts for Oxygen Reduction. *J. Am. Chem. Soc.* **2011**, *133*, 5182−5185.
(36) Rao, A. M.; Eklund, P. C.; Bandow, S.; Thess, A.; Smalley, R. E. Evidence for Charge Transfer in Doped Carbon Nanotube Bundles from Raman Scattering. *Nature* **1997**, *388*, 257−259.
(37) Cohen, E.; Dodiuk, H.; Ophir, A.; Kenig, S.; Barry, C.; Mead, J. Evidences for π-Interactions between Pyridine Modified Copolymer and Carbon Nanotubes and its Role as a Compatibilizer in Poly(methyl methacrylate) Composites. *Compos. Sci. Technol.* **2013**, *79*, 133−139.
(38) Lai, C.-H.; Wu, I.-C.; Kang, C.-C.; Lee, J.-F.; Ho, M.-L.; Chou, P.-T. Homogeneous, Surfactant-Free Gold Nanoparticles Encapsulated by Polythiophene Analogues. *Chem. Commun.* **2009**, 1996−1998.

DOI: 10.1021/acsami.5b01849
ACS Appl. Mater. Interfaces 2015, 7, 9841−9850